Alunite and natroalunite tell a story-the age and origin of Carlsbad Cavern, Lechuguilla Cave, and other sulfuric-acid type caves of the Guadalupe Mountains

Victor J. Polyak, W. C. McIntosh, Paula P. Provencio, and Necip Guven
2006, pp. 203-209. https://doi.org/10.56577/FFC-57.203

in:

Caves and Karst of Southeastern New Mexico, Land, Lewis; Lueth, Virgil W.; Raatz, William; Boston, Penny; Love, David L. [eds.], New Mexico Geological Society 57th Annual Fall Field Conference Guidebook, 344 p. https://doi.org/10.56577/FFC-57

This page is intentionally left blank to maintain order of facing pages.

ALUNITE AND NATROALUNITE TELL A STORY – THE AGE AND ORIGIN OF CARLSBAD CAVERN, LECHUGUILLA CAVE, AND OTHER SULFURIC-ACID TYPE CAVES OF THE GUADALUPE MOUNTAINS

VICTOR J. POLYAK[1], WILLIAM C. McINTOSH[2], PAULA P. PROVENCIO[3], AND NECIP GÜVEN[4]
[1]Earth and Planetary Sciences, University of New Mexico, 200 Yale Blvd., Northrop Hall, Albuquerque, NM 87131
[2]New Mexico Bureau of Mines and Mineral Resources, New Mexico Tech, 801 Leroy Place, Socorro, NM 87801
[3]Sandia National Laboratories, Albuquerque, NM 87185
[4]Department of Geosciences, Box 41053, Texas Tech University, Lubbock, TX 79409

Abstract.— Sulfate minerals alunite, natroalunite, hydrobasaluminite, and gypsum, produced from sulfuric-acid speleogenesis, are essential to the story of the origin of Carlsbad Cavern, Lechuguilla Cave, and many other major caves of the Guadalupe Mountains, southeastern New Mexico. Alunite is particularly important not only because it is a byproduct of sulfuric acid cave genesis, but because it contains telling isotopic signatures of sulfur, oxygen, hydrogen, potassium, and argon. Alunite has been reliably dated using the $^{40}Ar/^{39}Ar$ method yielding the timing of sulfuric-acid speleogenesis for Carlsbad Cavern, Lechuguilla Cave, and other sulfuric-acid caves as well as uplift and canyon incision rates for the Guadalupe Mountains. The repeatability of the $^{40}Ar/^{39}Ar$ results was demonstrated from analyses of alunite aliquots processed three different ways: 1) non-chemical alunite separation by simple gravity-method in water, 2) chemical separation using HF, 1 & 2 were not encapsulated for irradiation; and 3) encapsulation of HF-treated aliquots for irradiation. In addition to the chronology, negative sulfur isotope values for the alunite strongly point to a microbial-related process, and both alunite and natroalunite occur as micrometer-sized cube-like rhombs, an indicator of a low temperature origin of these large caverns. Larger ***a*** dimensions of the unit-cells of relatively well-formed alunite from the caves (determined by X-ray diffraction) are similar to those of synthetic alunites produced in the laboratory at <100ºC, and also support a low-temperature origin. Stable isotope values of the oxygen and hydrogen in the alunite have potential to generate more accurate values for the temperature and isotopic character of water in which the caves were formed. Timing of speleogenesis determined by $^{40}Ar/^{39}Ar$ dating of alunite shows this process was active as far back as ~12 Ma and slowly migrated eastward for at least 8-9 Ma up to 3-4 Ma ago. Rio Grande Rift faulting and tilting of the Guadalupe block during this period is probably the eastward-driving mechanism. If sulfuric-acid speleogenesis is taking place today, it is most likely happening east of the Guadalupe Mountains in the subsurface.

INTRODUCTION

Sulfuric acid speleogenesis is a distinctive cave-forming process that leaves behind tell-tale by-products, in contrast to the more common carbonic acid cave-forming process that essentially leaves nothing but space (Sasowsky, 1998). Consequently, by-products of sulfuric acid speleogenesis are unique in that they can be studied to determine the absolute timing of speleogenesis, and to reconstruct the environment of speleogenesis. The big caves of the Guadalupe Mountains (Fig. 1) in southeastern New Mexico formed by this H_2S-H_2SO_4-related process (Hill, 1987) and accordingly the age and origin of these caves could be determined (Polyak et al. 1998). The byproduct materials of sulfuric acid cave origin include gypsum ($CaSO_4•2H_2O$), alunite ($KAl_3(SO_4)_2(OH)_6$), natroalunite ($NaAl_3(SO_4)_2(OH)_6$), jarosite ($KFe_3(SO_4)_2(OH)_6$), aluminite ($Al_2(SO_4)(OH)_4•7H_2O$), hydrobasalumite ($Al_4(SO_4)(OH)_{10}•12\text{-}36H_2O$), hydrated halloysite ($Al_2Si_2O_5(OH)_4•2H_2O$), quartz, amorphous silica, Fe- and Mn-oxides, Al-hydroxides, hydrous Fe-sulfates, and elemental sulfur (Polyak and Provencio, 2001). The study of all of these has potential to contribute information about the history of speleogenesis, but alunite is the most useful of the by-products.

Alunite was first reported in the Guadalupe Mountains caves in Lechuguilla Cave (Palmer and Palmer, 1992), and alunite and natroalunite were reported in Carlsbad Cavern soon after that (Polyak and Güven, 1996). Since then alunite in datable quantities has been found in three additional caves: Endless, Cottonwood, and Virgin (Polyak and Provencio, 2001). Aliquots of purified alunite were dated in 1998 using $^{39}Ar/^{40}Ar$ and the published results offered the timing and progression of sulfuric acid-related speleogenesis in the Guadalupe Mountains (Polyak et al., 1998). Further details of the sulfuric acid speleogenesis model were provided by Palmer and Palmer (2000) and complement the discussion of the potential of the study of alunite.

FIGURE 1. Photo showing the large entrance passage of Cottonwood Cave. These exceptionally large cave passages are difficult to explain using the more traditional carbonic acid speleogenesis models in such a dry environment.

All samples of alunite and natroalunite from the Guadalupe Mountains caves are comprised of micrometer-sized pseudocube rhombs. With the exception of an alunite occurrence in Lechuguilla Cave having crystal sizes up to 20 µm in diameter, all other occurrences were comprised of crystals less than 5 µm and typically 1-2 µm. The alunite in all cases was associated with hydrated halloysite. The deposits are generally white and chalky in appearance. Manganese oxides are commonly associated with these deposits. Alunite is found in cave areas protected from drip or flood waters as wall residues, pockets of altered bedrock, solution cavities, and floor deposits.

We discuss the significance of alunite to the age and origin of Carlsbad Cavern, Lechuguilla Cave, and three other caves in the Guadalupe Mountains. A brief review of the mineral assemblage associated with alunite is offered to support the presence of a H_2S-H_2SO_4 cave-forming environment. Alunite was synthesized at relatively low temperature to better understand the conditions necessary for its formation during speleogenesis. The reliability of the age data is discussed as well, especially in terms of the analyses performed and tests conducted that show the percent of ^{39}Ar escape from the fine-grained crystals of alunite during irradiation. These age data compare well with more recent work done on the Rio Grande Rift (Lueth et al. 2005) and invite discussion on the importance of the comparison of the evolution of the Rio Grande Rift and caves of the Guadalupe Mountains. We also seek to convey that other information can be retrieved from the study of alunite, particularly from its stable isotope geochemistry (Rye et al., 1992), and that most of the potential for further studies still remain.

METHODS

Mineral assemblage identification

All minerals in the alunite-associated assemblage and synthesized materials for comparison were identified using X-ray diffraction (XRD). The minerals alunite, natroalunite, jarosite, gypsum, hydrobasaluminite, aluminite, hydrated halloysite, and quartz were separated, X-rayed, and indexed at the Clay Laboratory at Texas Tech University for positive identification. Support for mineral identification was provided using scanning (SEM) and transmission (TEM) electron microscopy and energy dispersive X-ray spectroscopy (EDX) at Texas Tech University and Sandia National Laboratories. A detailed mineral assemblage associated with alunite and H_2S-H_2SO_4-related cave genesis is given in Polyak and Provencio (2001). All aliquots of alunite that were dated were checked for purification using XRD and TEM.

$^{39}Ar/^{40}Ar$ dating of cave alunite

15 to 50 mg aliquots of purified cave alunite were irradiated in vacuo with interlaboratory standard Fish Canyon Tuff sanidine as a neutron fluence monitor. The separates of alunite were incrementally heated in a double-vacuum Mo-resistance furnace in 7-10 steps at temperatures of 500-750°C. Argon isotopic compositions were measured with a MAP 215-50 mass spectrometer at the New Mexico Geochronology Research Laboratory at New Mexico Tech. Plateau ages and associated 2 standard deviation uncertainties for samples with flat age spectra defined by two or more contiguous incremental steps were calculated using the error formula of Samson and Alexander (1987). The alunite separates were processed and analyzed three different ways. Alunite was purified non-chemically using gravity settling, where 1-2 µm-sized alunite crystals settle faster than the submicron-sized hydrated halloysite tubes. Aliquots of alunite were separated but still contained 1-5% hydrated halloysite (95 to 99% alunite). Samples were treated with 25% HF for about one hour, and this process removed all clay contaminates. Later, four sample aliquots, two separated by gravity settling and two HF-treated, were encapsulated in Pyrex tubes prior to irradiation to assess for ^{39}Ar recoil loss during the irradiation process. Argon expelled into the capsules during irradiation was analyzed after piercing the capsules with a CO_2 laser, then the alunite was extracted from the capsules and analyzed by resistance furnace incremental heating.

Alunite synthesis

Alunite and natroalunite were synthesized to better understand the origin of these minerals in the sulfuric acid cave-forming environment. The alunite was prepared at relatively low temperature and these precipitates were compared chemically and physically to alunite and natroalunite from these caves.

Potassium and sodium alunites were synthesized after the methods of Parker (1969). K-alunite was prepared by mixing K_2SO_4 and $Al_2(SO_4)_3$•$15.5H_2O$ solutions. Na-alunite was prepared by mixing Na_2SO_4•$5.7H_2O$ and $Al_2(SO_4)_3$•$15.5H_2O$ solutions. These salt solutions were slowly combined (adding alkali salts to the $Al_2(SO_4)_3$•$15.5H_2O$ solutions) and then digested at 50-90ºC for 30 minutes. The alkali sulfate solutions had pHs ranging from 5.9 to 7.8, depending on the amount of K_2SO_4 or Na_2SO_4•$5.7H_2O$. The $Al_2(SO_4)_3$•$15.5H_2O$ solutions had pHs ranging from 2.4 to 3.0. The salt solutions, when combined, quickly began to turn cloudy (visible indication of precipitation) and had measured pHs ranging from 2.6 to 3.1. Na-alunite solutions seemed to take longer to produce precipitates. The mixed salt solutions were continuously stirred at 95°C for four days, while pHs ranged from 1.9 to 2.3. After four days, solutions were quenched in a 20°C water bath and excess salt was washed from the samples with a centrifuge. A small aliquot of the reaction products was then examined with XRD and electron microscopy. The remainder of the reaction products was dried in an oven at <100°C. The powder was weighed to determine the approximate yield of the reaction. Two additional runs were prepared with sodium silicate solutions, one at pH=3 and the other at pH=6.

RESULTS

Chemistry of cave alunite and natroalunite

Alunite is associated with hydrated halloysite, and almost always found in cave areas containing remnant speleogenetic gypsum. Our data from the K and S sites, the $^{39}Ar/^{40}Ar$ ages and $\delta^{34}S$ values. The age data are offered later. Eleven alunite sam-

ples analyzed so far (from Carlsbad Cavern, Lechuguilla Cave, and Cottonwood Cave) have negative $\delta^{34}S$ values that range from -30 to 0 ‰. These sulfur isotope values are preliminary, and compare well with $\delta^{34}S$ values reported for speleogenetic elemental sulfur and gypsum from the same caves. The sulfur data is compiled and offered in Hill (1996).

Both alunite and natroalunite occur in these caves as a solid solution. Mole% natroalunite in these samples ranged from 86 to 5%, with most samples containing less than 50 mole% (Polyak and Güven, 1996). Figure 2 shows unit-cell dimensions of cave and synthetic alunite samples and Na- K- solid solution association as well as comparison of unit cell dimensions with stoichiometric and synthetic alunite and natroalunite.

Characteristics of synthetic alunite and natroalunite

Rapid precipitation (four days) of synthesized K-alunite and Na-alunite at 90°C resulted in crystals having different morphologies. Lower overall mineral yields were observed for Na-alunite, and higher yields were observed when excess K or Al was added to system. XRD and EDX results indicate that K-alunite is the dominant phase from initial solutions containing both Na and K, even when initial Na/K = 0.75. K-alunite preferentially precipitated over Na-alunite. Lattices for these low-temperature synthesized alunites were larger in the ***a*** dimension of the alunite unit cell than reported for stoichiometric ***a*** values, consistent with Alpers et al. (1992) and Stoffregen and Alpers (1992) who assigned the larger ***a*** dimension to incorporation of water into the lattice (hydronium alunite) shown in Figure 2. The TEM images show a large, but systematic variation in crystal size and morphology in the synthesized alunites. Most obvious is the difference in crystal size and morphology between Na-alunite and K-alunite. The synthesized Na-alunite produced cube-like rhombs up to 0.25 µm in diameter (Fig. 3). In contrast, synthesized K-alunite produced anhedral, subrounded to very irregular crystals

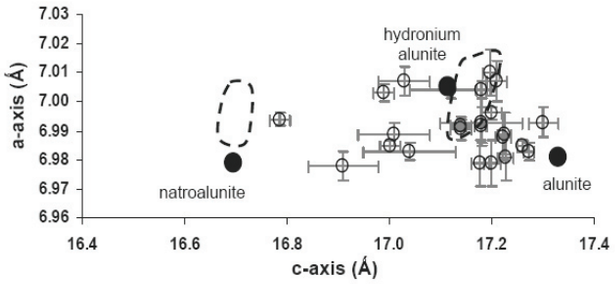

FIGURE 2. Graph showing the distribution of unit cell dimensions of cave and sysnthesized alunite and natroalunite. The large black circles are ideal unit cell dimensions taken from Stoffregen and Alpers (1992). The dashed-line areas encompass unit cell dimensions for synthesized alunite and natroalunite. The graph shows that most cave alunite has a high mole% K-alunite with dimensions similar to hydronium alunite.

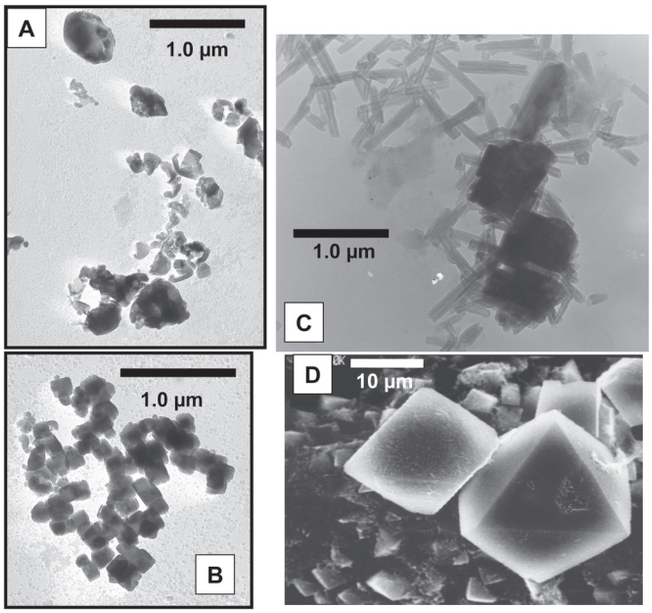

FIGURE 3. TEM and SEM micrographs showing synthesized and cave alunite crystals. **A.** Synthesized materials consisted of small irregular crystals of alunite and, **B**. rhomb-like crystals of natroalunite. **C**. Cave alunite is associated with hydrated halloysite (tubes). **D.** A deposit in Lechuguilla Cave near Glacier Bay produced large, well-formed alunite crystals.

up to 1.0 µm in diameter (Fig. 3). Crystal size increased with K content. The XRD data supports the EDX data and also indicates that K is preferentially utilized over Na during crystal growth.

$^{39}Ar/^{40}Ar$ geochronology

The alunite age results, published in Polyak et al. (1998) are summarized in Table 1. The ages show remarkable correlation with elevation, with older alunite ages from caves at higher elevation. Alunite collected from Cottonwood and Virgin caves, both located ~2000 m in elevation, had apparent ages of 11-12 Ma. Carlsbad and Lechuguilla caves yielded alunite from three different levels, from highest to lowest, ~6 Ma (1230-1250 m), ~5 Ma (1180 m), and ~4 Ma (1100 m). Alunite from Endless Cave, at the same elevation as Glacier Bay in Lechuguilla Cave, has an age of 6 Ma. $^{39}Ar/^{40}Ar$ analyses of these 95-99% alunite aliquots yielded flat plateau dates (Fig. 4). Similarly, the HF-treated alunite aliquots yielded flat plateau dates with slightly younger ages, but with essentially identical results. $^{39}Ar/^{40}Ar$ analyses of encapsulated alunite aliquots yielded flat plateau dates with the same results, and show that ^{39}Ar loss resulting from neutron irradiation is insignificant. These three sets of aliquots measured, (1) un-encapsulated alunite separated using gravity settling method, (2) un-encapsulated alunite separated chemically with HF, and (3) encapsulated alunite separated by gravity settling (n=2) and chemically with HF (n=2), yield essentially the same results and show the robustness of the $^{39}Ar/^{40}Ar$ dating of fine-grained cave alunite. Encapsulated results are offered in Figure 5 and Appendix 1.

TABLE 1. $^{39}Ar/^{40}Ar$ age data for alunite samples from five Guadalupe Mountains caves.

Cave	sample	elutriation age (Ma)	error	HF-treated age (Ma)	error	encapsulated age (Ma)	error	Recoil loss	Clay content
Carlsbad Cavern GCR	30HF			3.89	0.13				0%
Carlsbad Cavern NMR	29HF			3.98	0.13				0%
Carlsbad Cavern BR	28	4.00	0.04						3%
Carlsbad Cavern BR	27	4.07	0.07			4.12	0.04	2.3%	1-5%
Carlsbad Cavern NMR	29	4.50	0.16						10-15%
Endless Cave	02HF			6.02	0.05				0%
Endless Cave	02	6.34	0.23						5%
Endless Cave	02encap								0%
Lechuguilla Cave LL	18	5.16	0.13						1-5%
Lechuguilla Cave GB	32HF			5.72	0.08	5.99	0.01	4.5%	0%
Lechuguilla Cave GB	33a	6.07	0.08			6.09	0.07	2.1%	1-5%
Lechuguilla Cave GB	33b	6.02	0.06						3%
Lechuguilla Cave GB	33c	6.02	0.04						1%
Lechuguilla Cave GB	32	7.20	0.16						10-15%
Virgin Cave	20HF			11.30	0.17	11.88	0.09	1.8%	0%
Virgin Cave	20	11.92	0.16						5%
Virgin Cave	20	12.22	0.16						5%
Cottonwood Cave	17	12.26	0.16						1-5%

GCR = Green Clay Room, NMR = New Mexico Room, BR = Big Room, LL = Lake LeBarge, GB = Glacier Bay.

DISCUSSION

The environment in which alunite formed is also the environment of speleogenesis. The associated mineral assemblage (Polyak and Provencio, 2001) and size and morphology of crystals suggest that the environment of speleogenesis was acidic and low temperature (Stoffregen and Alpers, 1992), consistent with the sulfuric acid speleogenesis model proposed for Carlsbad Cavern, Lechuguilla Cave and other major caves in the Guadalupe Mountains (Jagnow et al., 2000). Evidence for both subaqueous and subaerial gypsum, elemental sulfur, and passage morphology indicate that most speleogenesis took place near the water table (Buck, 1994; Palmer and Palmer, 2000). After the water table descended below the cave, the byproduct materials such as alunite remained in a stable environment suitable for long-term preservation in those cave areas protected from drip and flood waters. The post-speleogenetic subaerial environment was ideal for prevention of any alkali exchange in the fine-grained alunite, ensuring its appropriateness for radiometric dating. Aliquots of alunite subsamples, processed three different ways, yielded the same ages per subsample and further demonstrate the robustness of the age results. The overall $^{39}Ar/^{40}Ar$ dating of alunite from five caves show a strong correlation with elevation with greater alunite ages at higher elevation, yielding the timing of speleogenesis for four different levels in the Guadalupe Mountains (Polyak et al., 1998). A simple third-order polynomial curve fits that age data with a y-intercept at the current water table near the city of Carlsbad at an elevation of 950 m ($y = 6.2749x^2 + 11.999x + 950$; $n = 14$; $R^2 = 0.9937$), where x = age (Ma) and y = elevation (m). This curve may be used to estimate the timing of speleogenesis for all sulfuric acid caves in the Guadalupe Mountains. For instance, Slaughter Canyon Cave where alunite has not yet been found is located at ~1380 m, yielding an estimated timing of speleogenesis of 7 Ma from our curve (Fig. 6).

The byproduct materials of speleogenesis inherited elemental and isotopic signatures of the sulfuric acid cave-forming environment as the water table slowly descended through the strata in which the caves developed. The small cube-like alunite crystals are characteristic of low temperature environments (Stoffregen and Alpers, 1992). Rapid formation of synthetic natroalunite at 90ºC resulted in moderately well-formed crystals of natroalunite, unlike the poorly formed synthetic alunite. At much lower temperatures in the cave environment, well-formed rhombs of alunite and natroalunite probably needed a lengthy time to mature. Low temperature sulfuric acid speleogenesis at any definable passage level probably lasted thousands to tens of thousands of years (Palmer and Palmer 2001) resulting in ample time for cave alunite crystals to mature to well-formed cube-like rhombs, in contrast to the rapidly formed synthetic alunite. Also, alteration of aluminum-bearing materials such as clays are needed to provide the ingredients for alunite and natroalunite, and at low temperature, the time needed for this process was probably lengthy and required thousands and tens of thousands of years.

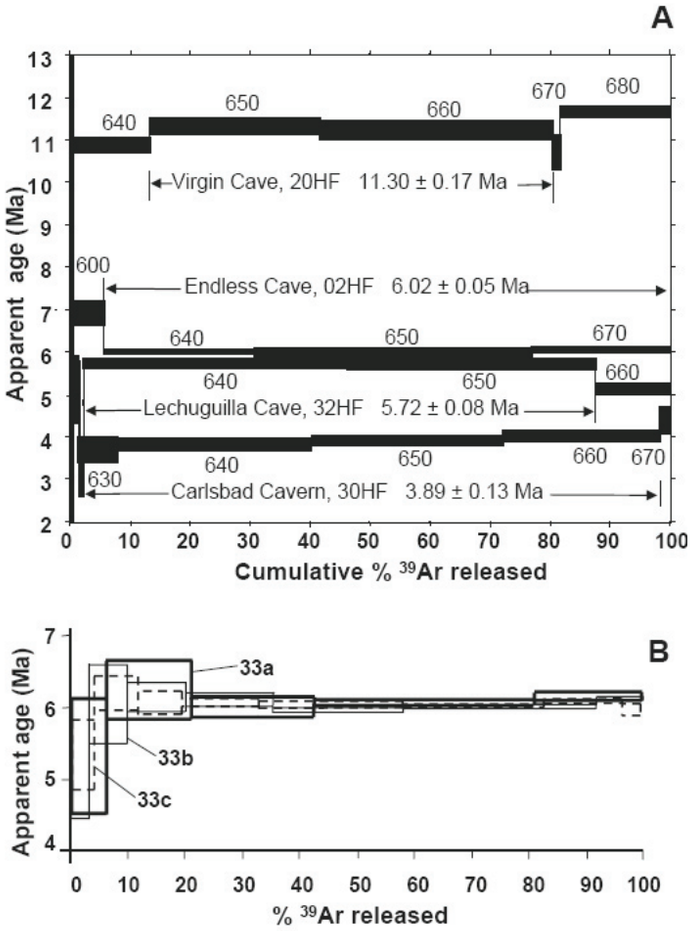

FIGURE 4. **A**. $^{40}Ar/^{39}Ar$ age spectra for samples treated with HF from each cave level (modified from Polyak et al., 1998). See Table 1. **B**. $^{40}Ar/^{39}Ar$ age spectra for three size-separates (a, b, c) of an alunite sample (33) from Lechuguilla Cave. The bold-lined spectra represents analysis of 33a having an average crystal diameter size of 1.5 µm. The fine-lined and dashed-lined spectra are plateaus from samples 33b (2.9µm) and 33c (8.3 µm), respectively. Results show that variation in crystal size does not affect age results.

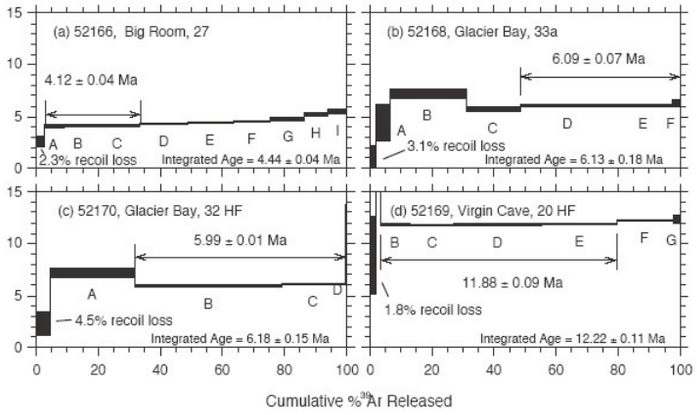

FIGURE 5. $^{40}Ar/^{39}Ar$ age spectra for samples that were vaccuum encapsulated during irradiation. The initial step of each spectrum is the analysis of the gas lost to the capsule during irradiation.

While alunite from five caves has been dated, little to no elemental and isotopic analyses have been done on the alunite or other byproduct materials, except for some sulfur analyses. The low $\delta^{34}S$ values (-30 to 0 ‰) thus far reported for alunite match those of the gypsum and elemental sulfur. They have been attributed to microbial reduction of sulfur in the subsurface Delaware Basin by Hill (1996). The three other stable isotope sites of these cave alunites ($\delta^{18}O_{SO4}$, $\delta^{18}O_{OH}$, and δD) have not yet been analyzed. These sites have potential to yield information about temperature of formation of alunite and paleo-groundwater $\delta^{18}O$ and δD values. In addition to these stable isotope sites, it is possible to extract Sr and Pb isotope values from the alunite, giving clues about the source materials responsible for the origin of the alunite.

Even though the H_2S source for speleogenesis (hydrocarbons in the Delaware Basin) differs from the sources of H_2S along the Rio Grande Rift responsible for ore production (sour gases from thermochemical reduction of Permian sulfate deposits; Lueth et al., 2005), the timing of these processes forming alunite (caves) and jarosite (ore deposits) is similar (last 10 Ma). The faults responsible for uplift of the Guadalupe block are on the eastern margin of the Rio Grande Rift. Lueth et al. (2005) noted that the pulses of sulfuric acid speleogenesis 11 Ma and 6-4 Ma reported by Polyak et al. (1998) correlate with timing of renewed tectonic activity in the Rio Grande Rift that formed jarosite. This suggests that the faults that uplifted the Guadalupe block were actively forming the Guadalupe Mountains as the caves were forming. The major episodes of speleogenesis represented by alunite ages of major cave levels at 4-6, and 11 Ma may correspond to these active periods of tectonic activity. Greater tectonic activity likely initiated movement of basinal fluids, forcing episodic pulses of H_2S to ascend into the Capitan Reef aquifer. If this is the case, the timing of uplift of the Guadalupe Mountains may be recorded by the caves. Each recorded episode of major speleogenesis (ie, the Big Room level) represents the position of the water table relative to the strata and shows a ~1000 m relative drop of the water table over the past 11 Ma. Overall results correspond to an uplift rate of the Guadalupe block greater than 90 m/Ma at the fault zone, comparable to the ~150 m/Ma uplift rate along the Rio Grande Rift determined by Lueth et al. (2005), with periods of major speleogenesis representing periods of greater tectonic activity. In addition to uplift rates, incision history can be retrieved from the alunite age data, which was compiled by DuChene and Martinez (2001) to determine average incision rates of ~70 m/Ma in the southwestern end of the mountains and ~20 m/Ma at the eastern end.

The location of the known significant sulfuric acid caves in the Guadalupe Mountains relative to elevation suggests that three distinct episodes of major speleogenesis took place (Fig. 6). The earliest, represented by numerous caves at higher elevations, took place from 12 to 10.5 Ma based on the location of big caves (Fig. 6). While alunite has not yet been found in the caves that represent the next episode (Slaughter Canyon caves), another important period of sulfuric acid speleogenesis occurred from about 7.8 to 7.5 Ma according to the age versus elevation formula presented above. The latest episode that formed Carlsbad Cavern and Lechuguilla Cave lasted from 6.2 to 3.8 Ma.

POTENTIAL FOR FURTHER RESEARCH

The study of speleogenetic alunite has offered considerable information about the timing of speleogenesis, details of the cave-forming environment, history of uplift of the Guadalupe Mountains and associated relative water table decline, and canyon incision rates. Even so, there still exists much potential for further study of cave alunite. Alunite is made up of several important elements that can produce isotopic information inherited from its environment of deposition. Reported isotopic signatures of alunite ($KAl_3(SO_4)_2(OH)_6$) include $^{39}Ar/^{40}Ar$ from K, $\delta^{34}S$ from the sulfur, $\delta^{18}O_{OH}$ from the oxygen in the OH, δD from the hydrogen

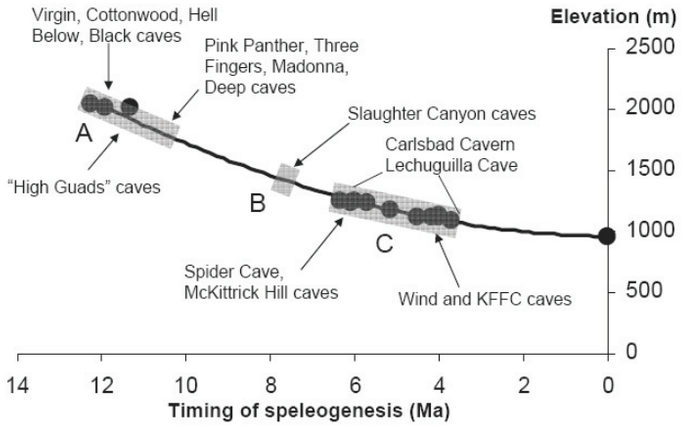

FIGURE 6. Graph showing trend of alunite ages relative to elevation. Also shown are three important periods of sulfuric acid speleogenesis represented by gray shaded areas along the curve (A = 10.5 to 12 Ma, B = 7.5 to 7.8 Ma, C = 3.8 to 6.2 Ma) and defined by the alunite ages and elevations of sulfuric acid caves.

in the OH, $\delta^{18}O_{SO4}$ from the oxygen in the SO_4 (Rye et al., 1992). The O and H isotopes have potential to yield temperature of formation and isotopic signature of the Miocene-Pliocene ground waters. Also, there might be potential for extracting environmental information from isotopic signatures of minor and trace elements such as Sr and Pb. Lastly, even the coarsely sampled sulfur isotope studies thus far are only prelude to important high resolution sulfur isotope studies of not only alunite, but jarosite, gypsum, elemental sulfur, hydrous Fe-sulfates, and hydrobasaluminite. The same applies to isotopic signatures of the other elements. Alunite has shown to be the most important of these by-products.

ACKNOWLEDGMENTS

We thank Ransom Turner of the Lincoln National Forest Service, Dale Pate, Jason Richards, and Stan Allison of the Carlsbad Caverns National Park, and Jim Goodbar of the Carlsbad District Bureau of Land Management for field assistance and for permission to collect samples used for this research.

REFERENCES

Alpers, C. N., Rye, R. O., Nordstrom, D. K., White, L. D., and King, B.-S., 1992, Chemical, crystallographic and stable isotopic properties of alunite and jarosite from acid-hypersaline Australian lakes: Chemical Geology v. 96, p. 203-226.

Buck, M. J., Ford, D. C., and Schwarcz, H. P., 1994, Classification of cave gypsum deposits derived from oxidation of H_2S, *in* Sasowsky, I. D. and Palmer, M. V., eds., Breakthroughs in Karst Geomicrobiology and Redox Geochemistry: Special Publication 1, p. 5-9.

DuChene, H. R. and Martinez, R., 2001, Post-speleogenetic erosion and its effect on caves in the Guadalupe Mountains, New Mexico and west Texas, Journal of Cave and Karst Studies, v. 62 (2), p. 75-79.

Hill, C. A., 1987, Geology of Carlsbad Cavern and other caves in the Guadalupe Mountains, New Mexico and Texas: New Mexico Bureau of Mines and Mineral Resources, Bulletin 117, 150 p.

Hill, C. A., 1996, Geology of the Delaware Basin, Guadalupe, Apache, and Glass Mountains, New Mexico and west Texas: Permian Basin Section-SEPM Publication 96-39, 480 p.

Jagnow, D. H., Hill, C. A., Davis, D. G., DuChene, H. R., Cunningham, K. I., Northup, D. E., and Queen, M. J., 2000, History of sulfuric acid theory of speleogenesis in the Guadalupe Mountains, New Mexico: Journal of Cave and Karst Studies, v. 62, p. 54-59.

Lueth, V. W., Rye, R. O., and Peters, L., 2005, "Sour gas" hydrothermal jarosite: ancient to modern acid-sulfate mineralization in the southern Rio Grande Rift: Chemical Geology, v. 215, p. 339-360.

Palmer, M.V. and Palmer, A. N., 1992, Geochemical and petrologic observations in Lechuguilla Cave, New Mexico, *in* Ogden, A.E., ed., Friends of Karst Meeting, Tennessee Technical University, Cookesville, TN, p. 25-26.

Palmer, A. N. and Palmer, M. V., 2000, Hydrochemical interpretation of cave patterns in the Guadalupe Mountains, New Mexico: Journal of Cave and Karst Studies, v. 62, p. 91-108.

Parker, R. L., 1969, Isomorphous substitution in natural and synthetic alunite: The American Mineralogist, v. 47, p. 127-136.

Polyak, V. J. and Provencio, P. P. 2001, Byproduct materials related to H_2S-H_2SO_4-influenced speleogenesis of Carlsbad, Lechuguilla, and other caves of the Guadalupe Mountains, New Mexico: Journal of Cave and Karst Studies, v. 63, p. 23-32.

Polyak, V. J., McIntosh, W. C., Provencio, P., and Güven, N., 1998, Age and Origin of Carlsbad Caverns and related caves from $^{40}Ar/^{39}Ar$ of alunite: Science, v. 279, p. 1919-1922.

Polyak, V. J. and Güven, N., 1996, Alunite, natroalunite, and hydrated halloysite in Carlsbad Cavern and Lechuguilla Cave, New Mexico: Clays and Clay Minerals, v. 44, p. 843-850.

Rye, R. O., Bethke, P. M., and Wasserman, M. D., 1992, The stable isotope geochemistry of acid sulfate alteration: Economic Geology, v. 87 (2), p. 225-262.

Samson S. D. and Alexander Jr. E. C., 1987, Calibration of the interlaboratory ^{40}Ar-^{39}Ar dating standard MMhb-1: Chemical Geology (Isotope Geoscience Section) v. 66, p. 27.

Sasowsky, I. D., 1998, Determining the age of what is not there: Science, v. 279, p. 1874.

Steiger, R. H., and Jäger, E., 1977, Subcommission on geochronology: Convention on the use of decay constants in geo- and cosmochronology: Earth and Planetary Science Letters, v. 36, p. 359-362.

Stoffregen, R. E. and Alpers, C. N., 1992, Observations on the unit-cell dimensions, H2O contents, and δD values of natural and synthetic alunite: American Mineralogist, v. 77, p. 1092-1098.

APPENDIX 1. Analytical data for encapsulated samples and Figure 5.

	ID	Power (Watts)	$^{40}Ar/^{39}Ar$	$^{37}Ar/^{39}Ar$	$^{36}Ar/^{39}Ar$ (x 10^{-3})	$^{39}Ar_K$ (x 10^{-15} mol)	K/Ca	$^{40}Ar^*$ (%)	^{39}Ar (%)	Age (Ma)	±1σ (Ma)
	VPC96027;252 #19, NM-136, 13.88 mg alunite, J=0.0038702±0.09%, D=1.00535±0.00031, NM-136, Lab#=52166-01										
x	Z	0	14.01	0.0272	46.11	5.58	18.7	2.7	2.3	2.65	0.24
	A	2	2.425	0.0037	6.139	15.6	138.1	24.5	8.8	4.09	0.06
	B	3	1.384	0.0032	2.600	23.4	157.2	43.5	18.6	4.12	0.04
	C	4	1.224	0.0028	2.056	36.2	181.1	49.4	33.7	4.12	0.02
x	D	5	1.224	0.0030	1.981	36.3	170.6	51.2	48.9	4.28	0.03
x	E	6	1.282	0.0032	2.130	34.5	160.4	50.0	63.3	4.38	0.03
x	F	7	1.403	0.0033	2.462	29.1	152.6	47.3	75.5	4.54	0.04
x	G	8	1.510	0.0038	2.702	26.9	133.8	46.3	86.7	4.79	0.06
x	H	9	2.050	0.0056	4.295	17.7	91.5	37.4	94.1	5.27	0.08
x	I	10	1.988	0.0057	3.994	14.2	89.3	39.9	100.0	5.46	0.11
	Integrated age ± 2σ			n=10		239.5	124.0	K2O=1.71%		4.44	0.04
	Plateau ± 2σ	steps A-C		n=3	MSWD=0.11	75.1	164.8±43.1		31.4	4.12	0.04
	VPH96033A al, #23,306*OR:136, alunite, J=0.0039146±0.08%, D=1.00535±0.00031, NM-136, Lab#=52168-02										
x	Z	0	30.51	0.0220	102.7	3.03	23.2	0.5	2.1	1.16	0.53
x	A	450	33.80	0.0148	112.2	6.42	34.4	1.9	6.7	4.41	0.89
x	B	490	15.41	0.0076	48.61	34.3	66.7	6.6	30.8	7.19	0.25
x	C	500	3.045	0.0079	7.440	25.2	64.9	27.2	48.6	5.79	0.09
	D	505	1.427	0.0067	1.812	43.4	75.6	61.8	79.1	6.11	0.04
	E	510	1.002	0.0062	0.4006	26.3	82.1	87.9	97.7	6.05	0.04
	F	515	1.093	0.0072	0.6101	3.33	70.9	83.2	100.0	6.26	0.13
	Integrated age ± 2σ			n=7		142.1	65.7	K2O=1.45%		6.13	0.18
	Plateau ± 2σ	steps D-F		n=3	MSWD=1.32	73.1	77.7 ±11.3		51.4	6.09	0.07
	96032 al, #25,36*IR:136, alunite, J=0.00385±0.09%, D=1.00535±0.00031, NM-136, Lab#=52170-02										
x	Z	0	54.03	0.0089	181.7	9.45	57.4	0.6	4.5	2.30	0.59
x	A	500	13.32	0.0020	41.47	58.2	249.3	7.8	31.9	7.22	0.21
	B	510	1.065	0.0013	0.6066	99.9	386.7	82.8	79.0	5.97	0.02
	C	520	1.050	0.0013	0.4990	43.7	387.0	85.6	99.6	6.08	0.03
x	D	530	1.922	0.0047	2.391	0.821	108.1	62.8	100.0	8.26	0.53
	Integrated age ± 2σ			n=5		212.1	273.0	K2O=1.88%		6.18	0.15
	Plateau ± 2σ	steps B-C		n=2	MSWD=12.02	143.6	386.8±0.5		67.7	5.99	0.10
	96020 al, #24,324*OR:136, alunite, J=0.0039369±0.08%, D=1.00535±0.00031, NM-136, Lab#=52169-02										
x	Z	0	155.8	0.0327	522.9	2.43	15.6	0.8	1.8	8.82	1.89
x	A	450	57.77	0.0045	179.8	2.19	114.3	8.0	3.4	32.40	1.25
	B	470	2.830	0.0072	3.831	12.9	70.7	59.7	12.8	11.85	0.10
	C	490	2.149	0.0068	1.553	19.6	75.4	78.4	27.1	11.79	0.06
	D	495	2.059	0.0068	1.224	38.8	75.1	82.2	55.6	11.84	0.05
	E	500	2.016	0.0064	1.012	33.0	79.2	85.0	79.7	11.98	0.05
x	F	505	1.965	0.0056	0.7297	24.7	91.6	88.9	97.8	12.21	0.06
x	G	510	2.106	0.0088	1.113	3.01	57.7	84.2	100.0	12.40	0.18
	Integrated age ± 2σ			n=8		136.6	73.0	K2O=1.79%		12.22	0.11
	Plateau ± 2σ	steps B-E		n=4	MSWD=2.61	104.2	75.9 ±6.9		76.3	11.88	0.09

Notes:

Isotopic ratios corrected for blank, radioactive decay, and mass discrimination, not corrected for interfering reactions.
Errors quoted for individual analyses include analytical error only, without interfering reaction or J uncertainties.
Integrated age calculated by summing isotopic measurements of all steps.
Integrated age error calculated by quadratically combining errors of isotopic measurements of all steps.
Plateau age is inverse-variance-weighted mean of selected steps.
Plateau age error is inverse-variance-weighted mean error (Taylor, 1982) times root MSWD where MSWD>1.
Plateau error is weighted error of Taylor (1982).
Decay constants and isotopic abundances after Steiger and Jäger (1977).
symbol preceding sample ID denotes analyses excluded from plateau age calculations.
Weight percent K_2O calculated from ^{39}Ar signal, sample weight, and instrument sensitivity.
Ages calculated relative to FC-2 Fish Canyon Tuff sanidine interlaboratory standard at 28.02 Ma
Decay Constant (LambdaK (total)) = 5.543e-10/a
Correction factors:
$(^{39}Ar/^{37}Ar)_{Ca}$ = 0.0007 ± 5e-05
$(^{36}Ar/^{37}Ar)_{Ca}$ = 0.00027 ± 2e-05
$(^{36}Ar/^{39}Ar)_K$ = 0.01077
$(^{40}Ar/^{39}Ar)_K$ = 0.0257 ± 0.0013


Stop 4/Day 1 2005